Functional hybrids based on biogenic nanofibrils and inorganic nanomaterials

Bernd Wicklein[ab] and German Salazar-Alvarez[*ab]

This feature article reviews some of the recent work on the fabrication of functional hybrids based on biogenic nanofibers and inorganic nanomaterials with an emphasis on their functional properties and suggested potential applications. We also discuss some of the work oriented towards the formation of ordered materials in the pursuit of achieving a hierarchical construction. Besides the academic interest in biogenic nanomaterials, it is anticipated that the use of natural, abundant nanomaterials, *e.g.*, cellulose, chitin, collagen, and silk, could provide affordable functional nanomaterials in developing countries.

Introduction

In recent years, great research effort has been dedicated towards understanding the principles behind biological composites and their outstanding performance, given not only by their composition but also by their hierarchical structure across several length scales.[1] Understanding and mimicking the design principles of naturally occurring biocomposites is a formidable task of great scientific interest as it can pave the way to high performance materials.[2,3]

[a]*Materials and Environmental Chemistry, Arrhenius Laboratory, Stockholm University, SE-106 91 Stockholm, Sweden. E-mail: german@mmk.su.se*
[b]*Wallenberg Wood Science Center, KTH, SE-100 44 Stockholm, Sweden*

In parallel, with increased interest in alternatives to fossil fuels, there has been a strong move towards the fabrication of functional materials based on (fibrillar) biopolymers that can be extracted from renewable sources.[4,5] In this regard, four compounds stand out: (i) cellulose, the most abundant biopolymer present in the cell wall of green plants and algae; (ii) chitin, the next most abundant biopolymer present in insects, crustaceans, fungi, and diatoms; (iii) collagen, the most abundant protein in the animal kingdom present in most vertebrates, particularly in tendons, bones, skin, corneas, and cartilage; and (iv) silk, an old commodity protein used in textiles and medical sutures.[5,6] Additionally, there exist other fibrillar compounds of special scientific interest, *i.e.*, fibrils composed of amyloids[7] and viruses.[8] An overview of various methods to obtain these biogenic nanofibrillated (BNF) materials (shown in Fig. 1) is given in Table 1.

Bernd Wicklein graduated in 2007 from Stuttgart University with a degree in Materials Engineering. His diploma work was jointly conducted at Stockholm University under the supervision of Prof. L. Bergström and Prof. J. Bill. In 2011 he received his Ph.D. from the Autonomous University of Madrid in the group of Prof. E. Ruiz-Hitzky at the Materials Science Institute of Madrid (CSIC) in the field of bio-inspired interfaces. Then he continued in the same group with his postdoctoral work on thermostable influenza vaccines based on clay–lipid biohybrid materials. Since 2012 he has been a post-doctoral researcher in Prof. L. Bergström's group at Stockholm University devoted to nanocellulose hybrid materials.

German Salazar-Alvarez obtained his Bachelor's degree in 1999 from the Universidad Nacional Autónoma de México, a Ph.D. degree in 2005 from the Royal Institute of Technology (KTH), and his Docent degree from Stockholm University in 2012. During 2005–2007 he was a postdoc at the Universitat Autònoma de Barcelona and the Institut Català de Nano-tecnologia. Since 2010 he has been a group leader at Stockholm University. His research activities are devoted to the fabrication of new hybrid systems based on nanocellulose and functional nanoparticles as well as to the synthesis and structural characterisation of magnetic nanoparticles with anisotropic shapes and complex structures.

This journal is © The Royal Society of Chemistry 2013

J. Mater. Chem. A, 2013, **1**, 5469–5478 | **5469**
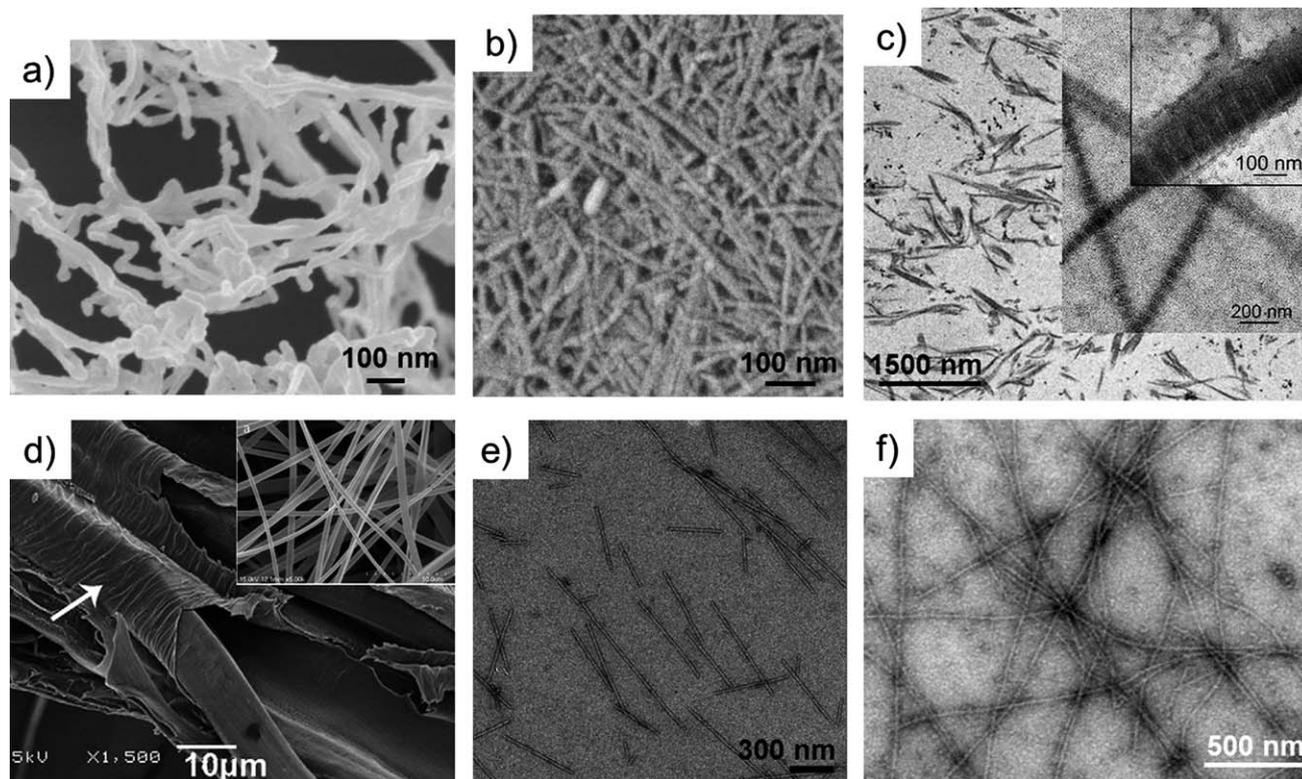
Fig. 1 Electron microscopy images of nanofibrillated cellulose from wood (a), chitin from a prawn (b), reprinted with permission from Ifuku et al.,[18] ©(2009) American Chemical Society; type I collagen from a rat tendon (c), reprinted with permission from Gobeaux et al.,[15] ©(2008) Elsevier; partially degummed native silkworm silk and electrospun fibroin nanofibers (d and inset), reprinted with permission from Sahoo et al.,[19] ©(2010) Elsevier; wild-type tobacco mosaic virus (e), reprinted with permission from Kadri et al.,[20] ©(2011) Elsevier; and β-lactoglobulin amyloid (f), reprinted with permission from Jones et al.,[21] ©(2010) American Chemical Society.

Table 1 Overview of biogenic nanofibrillated materials including source, dimensions, and chemical composition

Name	Typical source	Composition	D (nm)	L (μm)	Obtention
Nanofibrillated cellulose (NFC)	Wood, cotton, bacteria	Polysaccharide	3–30	0.1–0.8	Extraction from cell wall through mechanical treatment and/or enzymatic treatment[11,12]
Nanofibrillated chitin (NFChi)	Crab, squid	Polysaccharide	10–50	0.15–2.2	Fibers can be obtained through a simple grinding treatment in a never-dried state under an acidic condition after the removal of proteins and minerals[13,14]
Collagen fibril (CF)	Skin, bone, tissue	Protein	100	>1	Type I collagen molecules can be extracted from rat tail tendons, *in vitro* fibrillogenesis can render fibrils[15]
Silk filament (fibril) (SF)	Spider, silk worm	Protein	[a]	[a]	Extraction of silk fibers from the cocoons followed by dissolution in LiBr. Regenerated from spidroin and fibroin solution. See ref. 16
Amyloid fibril (AF)	Insulin, β-lactoglobulin	Protein	1–30	0.15–5	Assembly of proteins during incubation at typically 60 °C. The dimensions of the fibrils can be tailored using different incubation times[7,17]
Virus	Tobacco mosaic virus (TMV), potato virus X (PVX), bacteriophage M13, cowpea viruses (CVs)	Protein	7–18	0.3–0.86	For a review on the preparation of the different viruses, refer to ref. 8

[a] The dimensions are dependent on the processing.

5470 | J. Mater. Chem. A, 2013, **1**, 5469–5478

This journal is © The Royal Society of Chemistry 2013

Note that there are a few other systems based on proteins that also form nanoscale fibrillar structures, *e.g.*, elastin, keratin, or resilin, which are reviewed elsewhere.[9]

Bionanocomposites based on the fibrillar materials previously mentioned are an ideal component for the fabrication of multifunctional materials in combination with various useful inorganic nanomaterials as they can combine impressive properties with environmentally benign and energy efficient production routes.[10] In this feature article, we review some of the recent work on the fabrication of functional hybrids based on biogenic nanofibers and inorganic nanomaterials with an emphasis on their functional properties, formation of ordered structures, and suggested potential applications.

Functional hybrids

The growing interest in biogenic nanofibrils can be attributed to the improved characterization of the nanostructure of these and other biological materials and the chemical methods to tune their surface properties.[8,15,22] Biogenic nanofibers display a high surface density of functional groups as, for instance, amines on chitin, C6-hydroxyls on cellulose, amino acids on collagen, or cysteine groups on viruses. These functionalities permit site-specific chemistry and hence control over the affinity of the adsorbing species, *e.g.* polymer colloids,[23] drugs,[24,25] or enzymes.[26] Through the use of functional nanomaterials, the hybrids have found applications in many interesting areas. In this section we review some recent advances.

Energy and electron transport

Owing to the current interest of the scientific community in energy-related questions, there has been a tremendous amount of work directed towards the applications of novel hybrid materials as components in photovoltaics (PV), batteries, and field-effect transistors (FET).

For instance, Dang *et al.* constructed photoanodes for dye-sensitized solar cells through the templating of single-walled carbon nanotube (SWCNTs)–TiO_2 core–shell nanocomposites with a genetically engineered M13 virus (see Fig. 2).[27] They reported that the addition of small fractions of nanotubes improved the power conversion efficiency up to 10.6% by increasing the electron collection efficiency. Chiang *et al.* used genetically modified TMV to form current collectors and low light-reflecting surfaces.[28] Photoactive CuO was subsequently deposited by sputtering onto these patterned nanostructures, which were examined for photocurrent activity. A CuO thickness of 520 nm on TMV patterned current collectors produced a photocurrent density of 3.15 mA cm^{-2}, which is the highest yet reported for a similar sized CuO system. Bolisetty *et al.* fabricated a PV device using an amyloid–TiO_2 hybrid nanowire blended with polythiophene as an active layer (see Fig. 3).[29] They synthesized the hybrid structures by coating β-lactoglobulin amyloid protein fibrils with TiO_2 nanoparticles using titanium(IV) bis(ammonium lactato)dihydroxide as the precursor. The authors reported the current–voltage characteristics of the device, which had a fill factor of 0.53, a photovoltaic current
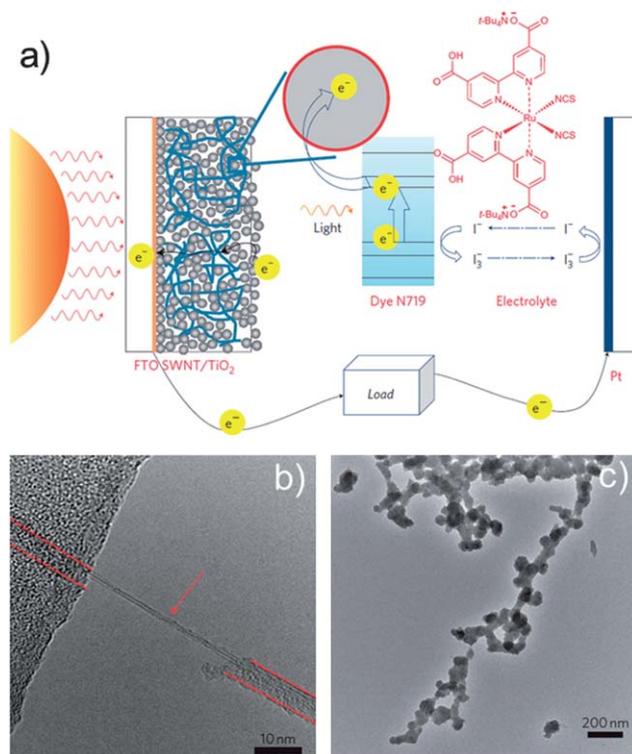
Fig. 2 (a) Scheme of the dye-sensitized solar cell incorporating the SWCNT–TiO_2 complex, (b) HRTEM image of a virus–SWCNT complex. A SWCNT is indicated by an arrow and the virus is indicated by dashed lines. (c) TEM micrograph of TiO_2 biomineralized on the virus–SWCNT complex. Adapted from Dang *et al.*,[27] with permission from Nature Publishing Group.
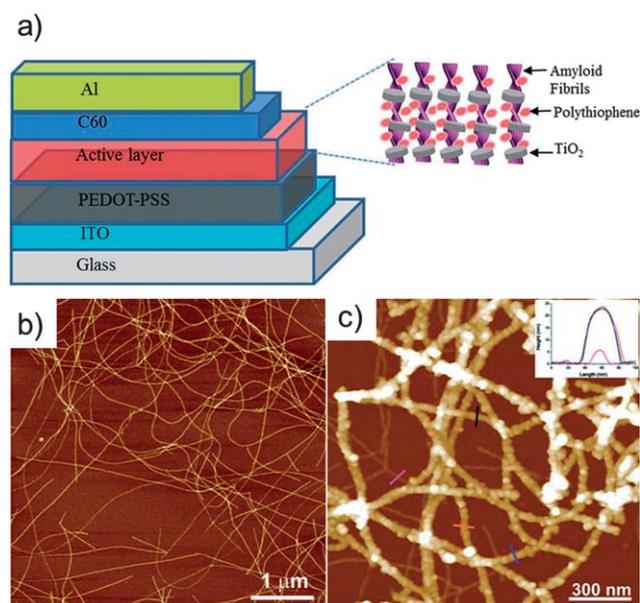
Fig. 3 (a) Schematic diagram of the hybrid photovoltaic device composed of the TiO_2–hybrid nanowires blended with polythiophene. (b) Atomic force microscope (AFM) image of the β-lactoglobulin AF showing long linear semiflexible structures. (c) AFM image of TiO_2 decorating the surface of the AFs. Reprinted with permission from Bolisetty *et al.*,[29] ©(2012) John Wiley & Sons.

This journal is © The Royal Society of Chemistry 2013

J. Mater. Chem. A, 2013, **1**, 5469–5478 | **5471**

density of 3.97 mA cm^{-2} and a power conversion efficiency of 0.72%.

Hybrids based on BNFs were tested also as components in batteries. Royston *et al.* produced a high area battery electrode by the electroless deposition of nickel and cobalt onto modified TMV templates that self-assemble vertically on gold patterned surfaces.[30] The incorporation of virus-assembled electrode surfaces into the nickel–zinc battery doubled the total electrode capacity. Hu *et al.* exploited the flexibility of nanopaper and fabricated a light-weight silicon-conductive device which was tested as a Li-ion battery anode.[31] The nanopaper consisted of highly porous nanocellulose-based aerogels with open channels and carbon nanotubes. Silicon was deposited using a plasma-enhanced CVD method. A stable capacity of 1200 mA h g^{-1} for 100 cycles in half-cells was achieved, well above the theoretical maximum of carbon but below that of silicon. The mechanical and optical properties of nanocellulose were exploited by Zhu *et al.* to fabricate an organic FET on a transparent and flexible nanopaper substrate.[32] The transistor consisted of SWCNTs serving as the transparent gate electrode, poly(methyl methacrylate) as the dielectric, and a naphthalenetetracarboxylic diimide derivative as the semiconductor. The authors found an effective charge carrier mobility value and on–off current ratio of 4.3×10^{-3} cm^2 V^{-1} s^{-1} and $I_{on/off} \sim 200$, respectively. Despite the somewhat reduced values, it should be emphasised that the flexibility of the device allowed a bending radius of 3.5 mm with *ca.* 10% decrease of the mobility. Alternatively, Atanasova and Rothenstein constructed an FET based on mineralised TMV virus with nanosized ZnO on a silicon dioxide-coated n-doped silicon substrate as the semiconducting, dielectric, and gate layers, respectively.[33] The authors reported values of the effective charge carrier mobility as high as 1.15×10^{-2} cm^2 V^{-1} s^{-1}, $I_{on/off} \sim 58\,700$, and a threshold voltage of +2.1 V.

Sensing and actuation

The combination of nanofibrillated biomaterials with functional entities led to interesting developments in analytical sensing and actuation. Mezzenga and co-workers combined graphene nanosheets and amyloid fibrils to create biodegradable, responsive, and well-organized lamellar structures.[34] The two compounds were assembled into water-stable colloids of graphene–amyloid hybrids which were further processed by vacuum filtration into conductive, lamellar films (Fig. 4a and b). These films demonstrated water-induced shape-memory effects that can be interesting in humidity sensing and micromechanics (Fig. 4c). The electric conductivity of the films was utilized in enzyme activity sensors measuring the hydrolysis of amyloid by pepsin. Another innovative amyloid-carbonaceous hybrid material has been recently presented by the same group. Herein, β-lactoglobulin amyloid fibrils were connected by sulfonated multiwalled carbon nanotubes (MWCNT) to form a pH responsive hydrogel.[35] At a pH below the isoelectric point of amyloid, pH < pH$_{iep}$, both components acquire opposing surface charges and gelling is induced by the formation of a highly interconnected network where one MWCNT connects several protein fibrils. This extraordinary connectivity
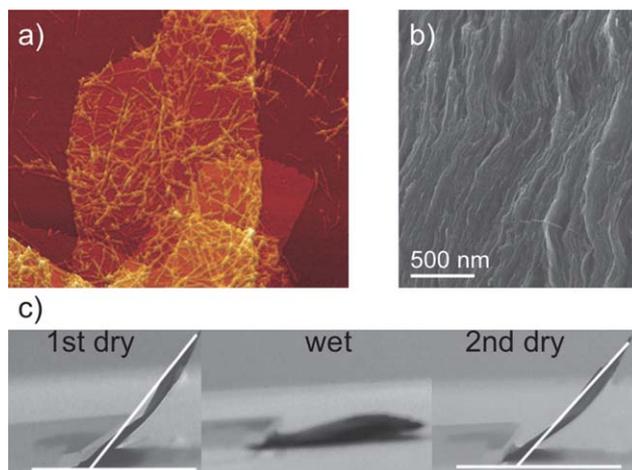
Fig. 4 (a) AFM image of a graphene–amyloid colloid. (b) SEM cross-section image of the hybrid nanocomposite showing complete exfoliation of graphene sheets by the amyloid fibrils and a well-organized layered structure. (c) Humidity-controlled shape-memory behavior of the hybrid nanocomposite film. Adapted from Li *et al.*,[34] with permission from Nature Publishing Group.

manifested itself in high storage moduli, while a rise in pH above pH$_{iep}$ caused the components to revert back to a fluid state. Such pH responsive, biocompatible hydrogels are thought to find application in drug release, sensors, and tissue engineering.

Nanofibrillated cellulose can also be used as biocompatible and non-degrading support for enzymes. The decoration of bacterial nanocellulose fibers (BNC) with gold nanoparticles (Au NPs) can yield a novel platform for bioelectroanalysis and bioelectrocatalysis through the immobilization of various kinds of heme enzymes.[36,37] In a synergistic fashion the Au NPs both ensured the capturing of the enzymes and enabled the electron transfer between the active protein center, the added mediator, and the electrode surface while BNC fibers provided the scaffold. Alternatively, by decorating bacterial cellulose nanofibers with hard ferrimagnetic CoFe$_2$O$_4$ nanoparticles, Olsson *et al.*[38] fabricated materials that could be actuated with a household magnet. Through a combination of freeze-drying or compression it was possible to form either a flexible magnetic aerogel or a stiff magnetic nanopaper, respectively. Tuning the concentration of the iron/cobalt solutions, the size and density of the nanoparticles could be controlled (see Fig. 5). Moreover, varying the composition of the nanoparticles to MnFe$_2$O$_4$ resulted in a soft ferrimagnetic material.

Biomedical applications

Nanofibrillated polysaccharides and proteins are also receiving growing attention for biomedical applications related to their biocompatibility, biodegradability, low toxicity, and mechanical strength. In this context, primary research fields are tailoring of biomedical nanoscaffolds, their employment for tissue and 3D cell culture, and nanofibrillated materials for the support and delivery of biomacromolecules.[39–41]

It has been recognized that optimal scaffolds mimicking extracellular matrices for tissue engineering and drug

5472 | *J. Mater. Chem. A*, 2013, **1**, 5469–5478

This journal is © The Royal Society of Chemistry 2013
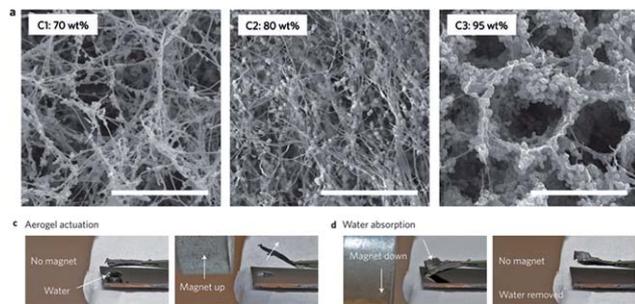
Fig. 5 Bacterial nanocellulose aerogel decorated with different concentrations of ferrimagnetic $CoFe_2O_4$ nanoparticles (upper panel). A piece of magnetic aerogel is held using tweezers and a small household magnet is used to bend the magnetic aerogel upwards (bottom left panel). The magnetic aerogel bends downwards in response to the magnet and absorbs the water droplet below, recovering its original shape upon removal of the magnet (bottom right panel). Adapted from ref. 38.

development should contain micro- and nanofibrillar compounds in analogy to their native equivalents.[42] Herein, silk fibroin filaments, collagen fibrils, BNC, elastin, and amyloids as the fibrous constituents are typically combined with suitable cross-linkers or polymers. Recent progress in nano-architecturing extracellular matrix components (ECMs) has been presented by Lu *et al.*, who prepared scaffolds of silk fibroin that self-assembled into nanofilaments, induced and controlled by the amount of added collagen fibrils.[43] The resultant scaffolds consisted of nanofibrous walls displaying macroporosity and biocompatibility that enabled the proliferation of cultured fibroblast cells. A layer-by-layer (LbL) approach was carried out by de Mesquita and coworkers to produce smooth, multilayered cellulose nanowhisker–collagen films with a regular bilayer thickness of 9.0 nm, making their possible employment as an extracellular matrix conceivable.[44] In other works, gelatin alone or in combination with hydroxyapatite was immobilized on a network of BNC.[45,46] Electrically stimulable ECMs for enhanced stem cell differentiation and proliferation were reported by Orza *et al.*, who coated gold on collagen fibrils that were subsequently deposited as LbL films (Fig. 6).[47] Nanofibrillated materials are also exploited in another rapidly developing area within biomedical applications, *e.g.* the support and delivery of biomacromolecules. The versatile surface chemistry of nanocellulose, *e.g.* epoxy, amine, or carboxylic acid functionalization, can be applied for the covalent conjugation of proteins, as shown by Arola *et al.* (Fig. 7).[48] These conjugates were spin-coated on silicon substrates to render bioactive and permselective films attributed to the tailorable nanoporous cellulose fiber networks.

Barrier coatings

A variety of technological applications ranging from flexible packaging to encapsulation of electronic components require highly transparent, flexible, and inexpensive high performance light and chemical barrier materials. A number of groups have combined nanoclays (*e.g.*, montmorillonite, MTM, and vermiculite, VER) and mica with nanocellulose to produce films
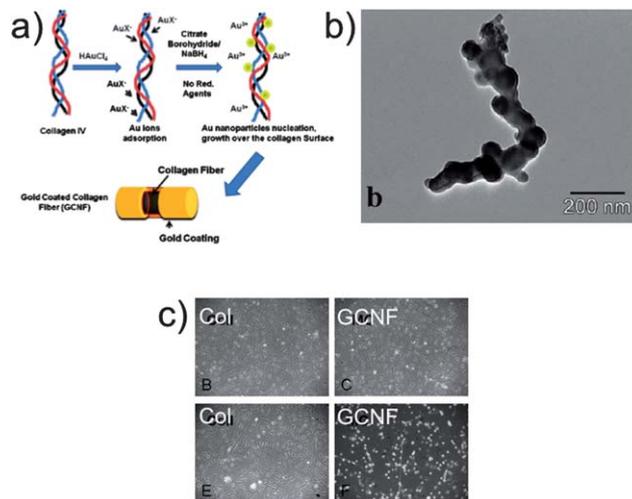
Fig. 6 (a) Schematic for the collagen nanofibers coated with thin layers of gold (GCNF). (b) TEM image of GCNF. (c) Phase contrast images of neuronal differentiation of mesenchymal stem cells with (bottom panels) and without electro-stimulation (top panels) with collagen (Col) substrates as controls. Adapted with permission from Orza *et al.*[47] (2011) ©American Chemical Society.
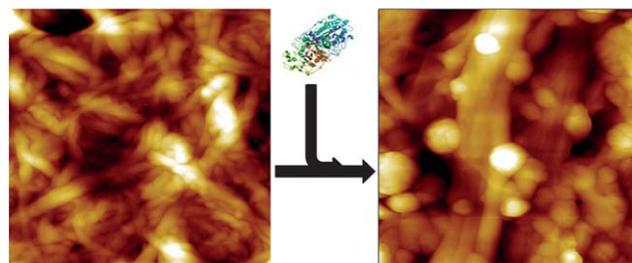
Fig. 7 AFM images before and after protein conjugation to NFC. Adapted with permission from Arola *et al.*[48] ©(2012) American Chemical Society.

with barrier properties. Wu *et al.* prepared transparent and flexible films based on anionic NFC–MTM hybrids with high mechanical properties and oxygen barrier properties.[49] The oxygen barrier performance was adjusted by varying the composition of the films: a composite film with 5% MTM had a Young's modulus of 18 GPa, tensile strength 509 MPa, work of fracture of 25.6 MJ m^{-3}, and oxygen permeability (OP) of 0.006 mL μm m^{-2} day^{-1} kPa^{-1} at 0% relative humidity. Increasing the inorganic content to 50% MTM resulted in an improved OP of 0.0008 mL μm m^{-2} day^{-1} kPa^{-1}, albeit with decreased light transmittance, tensile strength, and elongation at break. Aulin *et al.* prepared transparent and flexible films based on anionic NFC–VER hybrids with high mechanical properties and oxygen and water vapour barrier properties.[50] The resulting films were stiff, strong, and transparent, showing a tensile modulus of 17.3 GPa, strength up to 257 MPa, and transmittances higher than 60%. At 80% relative humidity, the material with 20% VER showed an OP and WVP of 1.5 mL μm m^{-2} day^{-1} kPa^{-1} and 21.2 mg μm m^{-2} s^{-1} kPa^{-1}, respectively. Ho *et al.* also investigated the mechanical behaviour and water vapour barrier performance of a number of hybrid films formed by 13 different clays and micas, although using instead *cationic*

NFC.[51] The authors found a remarkable water vapour barrier behaviour with a WVP as low as 0.025 mg µm m^{-2} s^{-1} kPa^{-1} using 50% inorganic content at 85% relative humidity. Regarding the mechanical properties, the hybrid with best barrier performance showed a tensile modulus, strength, and strain at break of 9.5 GPa, 104 MPa, and 1.9%, respectively, measured at 43% relative humidity (Fig. 8).

Structural applications

Many researchers have also aimed at exploiting the mechanical strength and lightness of BNF reinforced with inorganic nano-materials to fabricate porous foams with very low thermal expansion coefficients, high biocompatibility, and improved strength or hardness.

For instance, Cai et al. prepared cellulose–silica hybrid aerogels that have the mechanical strength and flexibility, large surface area, semi-transparency, and low thermal conductivity of the cellulose aerogels combined with mechanical integrity and heat insulation with a thermal conductivity as low as 0.025 W m^{-1} K^{-1}.[52] The hybrids were obtained through the impregnation of a nanoporous cellulose gel with tetraethyl orthosilicate and subsequent sol–gel formation and drying with supercritical CO_2. The tensile modulus and strength were determined as 72.0 MPa and 12.4 MPa for cellulose aerogel, and 48.2 MPa and 10.8 MPa for composite aerogel with 39% silica. Under compression deformation, the modulus and collapse stress were 12.0 MPa and 0.7 MPa for cellulose, and 7.9 MPa and 1.8 MPa for the composite (Fig. 9).

Following similar lines in bestowing NFC networks with high mechanical properties, Schütz et al. reported the formation of hard and transparent hybrid films of nanofibrillated cellulose and titania nanoparticles from aqueous dispersions.[53] The results show that limiting the titania nanoparticle
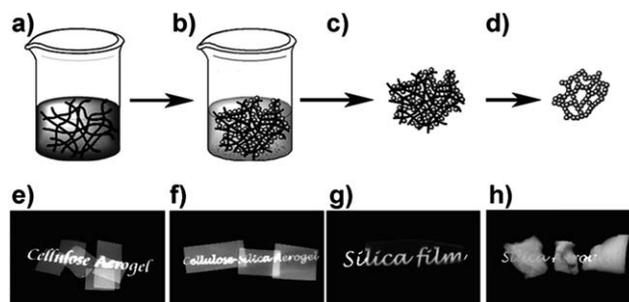

Fig. 9 Top: aerogel preparation. (a) Nanoporous cellulose gel with an interconnected nanofibrillar network is impregnated with silica precursor TEOS. (b) Silica formation by hydrolysis and condensation, giving cellulose–silica composite gel. (c) Drying with scCO$_2$ gives composite aerogel. (d) Calcination of cellulose leaves mesoporous silica aerogel. Bottom: macroscopic views of different cellulose–silica aerogels. Reprinted with permission from Cai et al.,[52] ©(2012) John Wiley & Sons.

concentration below 16 vol% yields homogeneous hybrids with a very high Young's modulus and hardness of up to 44 GPa and 3.4 GPa, respectively, and an optical transmittance above 80%. Electron microscopy shows that higher nanoparticle contents result in agglomeration and an inhomogeneous hybrid nanostructure with a concomitant reduction of hardness and optical transmittance. Infrared spectroscopy suggests that the nanostructure of the hybrids is controlled by electrostatic adsorption of the titania nanoparticles on the negatively charged nanocellulose surfaces.

A novel assembly approach to fabricate ultrathin robust free standing nanocomposite membranes was reported by Kharlampieva et al.[54] The materials are composed of a pre-cross-linked silk fibroin matrix with incorporated silica nanoparticles with silsesquioxane cores (POSS) or clay nanoplatelets. These reinforced silk membranes have enhanced mechanical properties as compared to traditional silk-based nanocomposites reported previously. Up to 6-fold and 8-fold increase in elastic modulus and toughness, respectively, were found for these nanocomposites. In contrast, traditional LbL-assembled nanocomposites showed only a 3-fold increase in mechanical strength. The obtained silk nanocomposites also revealed excellent optical transparency in the visible region especially if reinforced with POSS nanoparticles, which suggests their utility as low cost, nontoxic, and easily scalable reinforced biomaterials for mechanically demanding applications.

The structure of nacre and especially the role of interconnecting proteins in such natural nanocomposites inspired Laaksonen et al.[55] to engineer a bifunctional protein to assemble nanofibrillated cellulose onto graphene flakes. A hydrophobic protein group was connected to a cellulose-binding domain (Fig. 10). As a result, exfoliated graphene flakes could be stabilized in an aqueous suspension by NFC to prepare nanocomposite films that yielded excellent mechanical properties (20.2 GPa Young's modulus, 278 MPa tensile strength, and 57.9 kJ m^{-2} toughness) at a graphene content as low as 1.25%.

Biosilica was formed for the first time inside collagen fibrils through infiltration of polysilicic acid nanoparticles and
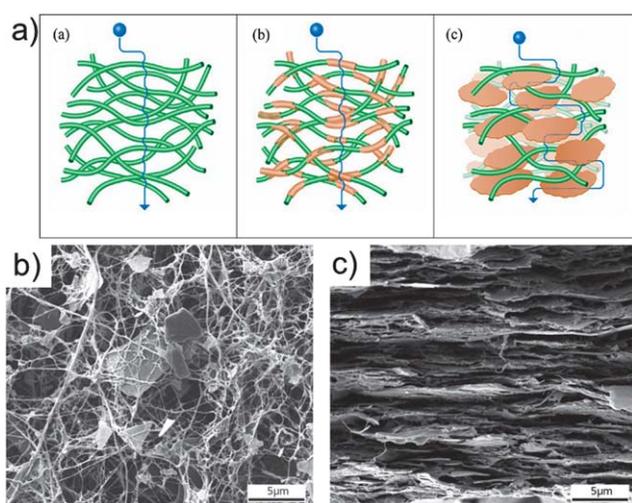
Fig. 8 (a) Schematic drawings of three model types including diffusion pathways: (a) neat NFC defined as "native network", (b) "covered fiber composite" model, and (c) the commonly used "fiber-brick composite" model. SEM images of (b) a dried suspension of NFC–mica, and (c) a fracture surface of the NFC–mica film cross-section. Adapted with permission from Ho et al.[51] (2012) American Chemical Society.
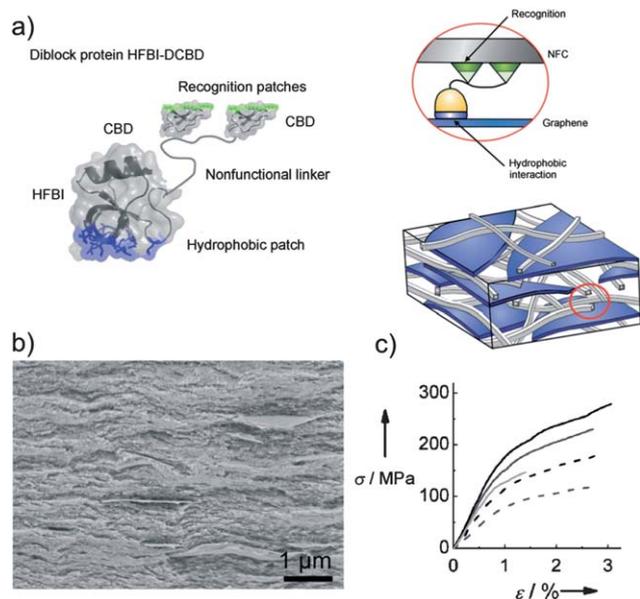
Fig. 10 (a) A schematic presentation of the layered composite structure showing the di-block fusion protein HFBI-DCBD (left) binding to graphene and NFC (right). (b) A SEM image of a cross-section of the NFC–HFBI-DCBD film with 20 wt% of graphene relative to NFC. (c) Stress–strain curves obtained for the sample shown in (b). The figure was adapted with permission from Laaksonen et al.,[55] ©(2012) John Wiley & Sons.

subsequent hydrolysis.[56] The templating collagen fibrils transferred their cross-banding pattern and microfibrillar architecture onto the amorphous silica, which can be transformed into crystalline silica after sintering. The resulting silica sponges could find application as a porous scaffold for bone repair and provide further insight into biosilification processes.

Absorbents

The formation of inexpensive porous structures with hydrophilic or hydrophobic surface behaviour can be utilized as well to absorb water or oils that could have a potential impact in water remediation. These structures can be particularly interesting when coupled to photocatalytic activity or an active retrieval system, i.e., magnetic attraction.

Highly porous, nanocellulose aerogels were formed by freeze-drying aqueous gels. TiO_2 coatings with thicknesses of about 7 nm were then deposited on the aerogel skeleton by chemical vapor deposition, as reported by Kettunen et al.[57] Such TiO_2-coated aerogel specimens essentially did not absorb water upon immersion. However, upon UV illumination, they absorb water 16 times their own weight and show a vanishing contact angle on the surface. Recovery of the original absorption and wetting properties could be obtained upon storage in the dark. The TiO_2-coated nanocellulose aerogels also show photo-oxidative decomposition, i.e., photocatalytic activity, which, in combination with the porous structure, is interesting for applications such as water purification. The wettability of nanocellulose networks was also explored by Olsson et al.[38] The hydrophilic open pore structure of bacterial nanocellulose scaffolds decorated with magnetic nanoparticles was exploited

to absorb water. The authors reported that 10 mg of pristine aerogel could take up to 1 g of water. Taking advantage of the magnetic and flexible properties of the aerogels, they used magnetic actuation to collect water, and subsequent squeezing of the aerogels released the absorbed water (see Fig. 5). Magnetic nanocomposites of collagen and superparamagnetic iron oxide nanoparticles (SPIONs) can be prepared by a simple process utilizing protein waste from the leather industry, as shown by Thanikaivelan et al.[58] Molecular interaction between helical collagen fibers and spherical SPIONs is proven through calorimetric, microscopic, and spectroscopic techniques. This nanocomposite exhibited selective oil absorption and magnetic tracking ability, allowing it to be used in oil removal applications. The environmental sustainability of the oil adsorbed bionanocomposite is also demonstrated here through its conversion into a bi-functional graphitic nanocarbon material via heat treatment. The approach highlights new avenues for converting bio-waste into useful nanomaterials in scalable and inexpensive ways.

Assembled structures

As shown in the previous section, the understanding and control of interactions and adsorption affinities between biogenic nanofibers and inorganic nanomaterials is of current interest as it has resulted in many interesting systems with various potential applications. However, the fabrication of well ordered systems based on BNFs, with all their structural benefits (i.e., mechanical, optical, etc.), is still lagging behind, with only a few systems being reported.

An illustrative example of organized nanofiber structures is achieved via ionic assembly, as reported by Wang et al., who assembled soft, cationic block copolymer micelles onto stiff, anionic NFC.[23] Herein, the controlled, opposite surface charges of the components drive the compounds into complexes of tailored size and shape.[23,25] Nanoscale lubrication afforded by the rubbery micelle cores improved the fracture toughness of the material, mimicking thus the alternating nanoscale hard/soft architecture found in many biological materials like nacre, bone, tooth enamel, or wood. Hierarchical networks are another interesting route to combine functionality and architecture. Namely, Aimé et al. reported a promising attempt to build hybrid networks by self-assembling of collagen–silica bio-nanohybrid particles where type I collagen was adsorbed on nanosized silica particles in a core–shell arrangement to render hybrid building blocks.[59] These blocks have been suggested to serve as nucleation centers for additional collagen fibrils via induced fibrillogenesis in order to bridge the building blocks to a network. These hybrids could find application as a bio-responsive device.

The use of liquid crystalline (LC) phases to structure materials has been recognized and is currently being expanded to some biogenic nanofibrils which are known to undergo a variety of LC phase transformations (see for instance ref. 60–62). Chung et al.[63] adapted this concept to obtain distinct supramolecular structures from biomimetic self-templating of liquid crystalline phases formed at the meniscus of an up-pulling

substrate from M13 phage solutions. In this way, iridescent films could be created with fibrous chiral M13 phages. Phage concentration and pulling velocity provided control over a variety of obtained chiral arrays and their optical properties. These oriented phage arrays were also used to direct the biomineralization of apatite to render tooth enamel-like organic–inorganic nanocomposites. LC phases have also been observed in nanocrystalline cellulose (NCC) obtained from wood.[64] These nematic LC phases of cellulose have been explored by MacLachlan's group to prepare ordered, mesoporous structures. They demonstrated, for the first time, the fabrication of chiral mesoporous silica by templating the cellulose liquid crystals with tetraethoxysilane and subsequent cellulose pyrolysis under air (see Fig. 11).[60] In a consecutive work, this chiral NCC–silica material was converted into free-standing mesoporous carbon films with nematic chirality by cellulose pyrolysis under nitrogen and silica removal in NaOH.[65] The former mesoporous materials have potential in photonic applications such as smart windows or enantioselective optical sensors due to their switchable iridescence and chirality, whereas the latter could find application as, for instance, supercapacitors.

Optical materials based on NCC hybrids were also presented by Olivier et al., who dispersed SWCNT with the help of cellulose nanocrystals that aligned to the SWCNTs supposedly driven by hydrophobic interactions.[66] Thin, multilayered films could be obtained from these stable hybrids in which the SWCNTs were well-dispersed and isolated within bilayers of NCCs. This feature is believed to be responsible for the observed NIR luminescence that could be profited from in the future in sensing applications as this optical phenomenon is highly sensitive to its local environment. Cellulose nanocrystals can also be complexed with cationic chitosan to form polyelectrolyte

Fig. 11 (a) Schematic of the chiral nematic ordering present in NCC and the pitch size, P. (b) Fingerprint texture characteristic of the chiral nematic ordering in NCC–silica precursor films (scale bar 100 μm). (c) Photograph showing the different colours of mesoporous silica films. (d) Side view of a cracked film showing the stacked layers that result from the helical pitch of the chiral nematic phase (scale bar 3 μm). The figure was adapted from Shopsowitz et al.,[60] with permission from Nature Publishing Group.

particles with potential application as drug delivery vehicles.[25] The titration direction of these two polyelectrolytes and the relative ratio of the two components provided control over their size and shape, ranging from a few hundred nanometers to several micrometers and from near spherical to rhombus and hexagonal-like morphologies.
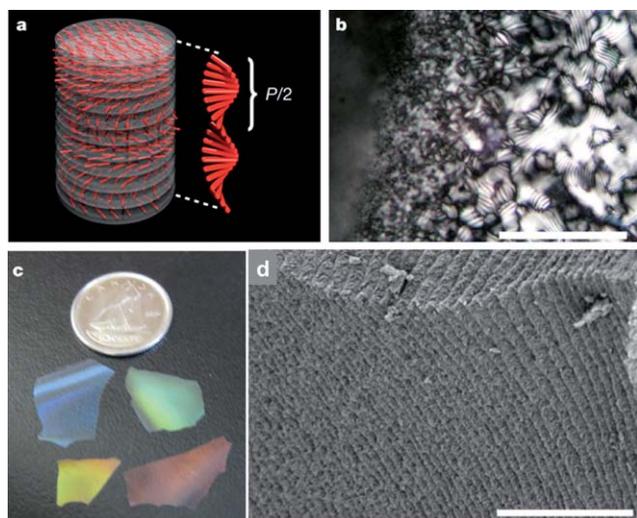
The formation of LC phases displayed by nanocrystalline cellulose and chitin needs to be investigated in more detail as similar ordering mechanisms could be present also in fibers.[67] This could pave the way for the fabrication of well ordered fiber-based components or fiber-reinforced LC phases.

Future outlook and perspective

The isolation and preparation of some biogenic nanofibrillated materials with precisely controlled dimensions and surface properties has fostered the development of fascinating new material concepts. However, in order to predict functions and structures of BNF-based assemblies, the characterization and tailoring of fiber–particle and fiber–fiber interactions are still of topical interest. One reason could be the huge variety of surface properties of a number of biogenic fibers, which depend on their fabrication route and source, even if they originate from the same biological family. Methods to characterize and control their dimensions and surface behaviour akin to the so-called "TEMPO oxidation", developed by Saito and Isogai,[22] are thus still needed.

Moreover, in comparison to synthetic or inorganic nanometric materials that have already left a remarkable footprint in nanoarchitectonics,[68,69] similar materials created from biological nanomaterials are still scarce. A large body of work concerning the assembly of the first two levels in nanoarchitectonics, e.g. molecular surface modification and assembly of nanoscaled entities, has been achieved, but the subsequent hierarchical level is often neglected. One approach to tackle this issue might be the implementation of programmable molecules like DNA or nucleotides for directed assembly of nanofibrillated biomaterials into designed architectures. Inspiring work on cellulose–DNA nanohybrids[70] and virus–DNA arrays through hydridization[71] has been presented but not continued to the best of our knowledge. The advent of DNA origami[72] and related programmed assemblies[73] could hence provide a stimulus and boost bio-nanoarchitectonics. Another route that has already been proposed for ceramic materials is the use of ice crystal templating, i.e., freeze-casting.[74]

The greatest benefit arising from the use of biogenic nanofibrillated materials is, in our opinion, their possible socio-economic impact on the advancement of developing countries as these nanoscale components are readily accessible and inexpensive. BNFs available from biomass, food waste, or through cultivation such as cellulose (wood, cotton), chitin (fungi, insects), collagen (animal skin) or silk (spider silk, worms) are present throughout the world. Moreover, their isolation and post-treatment are based on traditional mechanical and low-energy chemical processing rendering their production inexpensive. The availability of these biomaterials together with geogenic nanomaterials such as clays is expected

5476 | J. Mater. Chem. A, 2013, **1**, 5469–5478

This journal is © The Royal Society of Chemistry 2013

to facilitate the entry of developing countries into the nanoscience community without the need for high-cost infrastructure. Thus, local industries could benefit from producing and exporting value-added products using inexpensive approaches.

Conclusions

A fundamental leap in the deployment of BNFs in advanced materials has been the recognition of the synergetic benefits obtained from combining the outstanding inherent mechanical and optical properties with added artificial functionalities. The basis of this development has been the enormous progress in nanofiber characterization and functionalization by molecular or particulate entities, providing thus adequate linkers for high-order nanocomposites like fiber–nanoparticle conjugates, fiber–fiber assemblies, or fiber–sheet structures. Besides, templating strategies for functional nanocoatings have been further developed and fostered applications as varied as FETs or electrostimulating EMCs. However, there is still a need for continued focus and investigation on multi-scale structuring of bionanofiber-conjugates employing concepts such as e.g. programmed self-assembly or advanced processing routes like 3D printing, robo-printing, or ice templating. These strategies fall within the nanoarchitectonics approach to hierarchical materials and can be expected to lead to a great variety of advanced applications. Nature offers a wide range of nanofibrillated materials that have great potential for implementation in advanced functional hybrid concepts. BNFs from abundant sources, e.g., cellulose, chitin, collagen, and silk, can also offer tremendous opportunities for the developing world in areas such as agriculture, sustainability, and medicine, as they can be obtained at low cost and could have positive effects on the local industry. Furthermore, development of nanoscience and nanotechnology based on renewable materials can make a contribution to combat some of the global problems described in the UN Millennium Development Goals, such as environmental sustainability, eradicating extreme hunger, and water treatment and remediation.

Acknowledgements

References

1 P. Fratzl and R. Weinkamer, Prog. Mater. Sci., 2007, 52, 1263–1334.
2 P. Fratzl, J. R. Soc., Interface, 2007, 4, 637–642.
3 A. R. Studart, Adv. Mater., 2012, 24, 5024–5044.
4 A. Gandini, Green Chem., 2011, 13, 1061.
5 F. G. Omenetto and D. L. Kaplan, Science, 2010, 329, 528–531.
6 A. C. Neville, Biology of Fibrous Composites, Cambridge University Press, Cambridge, 1993.
7 J. Adamcik, J.-M. Jung, J. Flakowski, P. De Los Rios, G. Dietler and R. Mezzenga, Nat. Nanotechnol., 2010, 5, 423–428.
8 S. Lee, J. Lim and M. Harris, Biotechnol. Bioeng., 2011, 109, 16–30.
9 X. Hu, P. Cebe, A. S. Weiss, F. Omenetto and D. L. Kaplan, Mater. Today, 2012, 15, 208–215.
10 A. K. Mohanty, M. Misra and G. Hinrichsen, Macromol. Mater. Eng., 2000, 276–277, 1–24.
11 D. Klemm, F. Kramer, S. Moritz, T. Lindström, M. Ankerfors, D. Gray and A. Dorris, Angew. Chem., Int. Ed., 2011, 50, 5438–5466.
12 R. J. Moon, A. Martini, J. Nairn, J. Simonsen and J. Youngblood, Chem. Soc. Rev., 2011, 40, 3941–3994.
13 S. Ifuku and H. Saimoto, Nanoscale, 2012, 4, 3308–3318.
14 N. Lin, J. Huang and A. Dufresne, Nanoscale, 2012, 4, 3274–3294.
15 F. Gobeaux, G. Mosser, A. Anglo, P. Panine, P. Davidson, M.-M. Giraud-Guille and E. Belamie, J. Mol. Biol., 2008, 376, 1509–1522.
16 H.-J. Jin and D. L. Kaplan, Nature, 2003, 424, 1057–1061.
17 R. Jansen, W. Dzwolak and R. Winter, Biophys. J., 2005, 88, 1344–1353.
18 S. Ifuku, M. Nogi, K. Abe, M. Yoshioka, M. Morimoto, H. Saimoto and H. Yano, Biomacromolecules, 2009, 10, 1584–1588.
19 S. Sahoo, S. L. Toh and J. C. H. Goh, Biomaterials, 2010, 31, 2990–2998.
20 A. Kadri, E. Maiss, N. Amsharov, A. M. Bittner, S. Balci, K. Kern, H. Jeske and C. Wege, Virus Res., 2011, 157, 35–46.
21 O. G. Jones, J. Adamcik, S. Handschin, S. Bolisetty and R. Mezzenga, Langmuir, 2010, 26, 17449–17458.
22 A. Isogai, T. Saito and H. Fukuzumi, Nanoscale, 2011, 3, 71–85.
23 M. Wang, A. Olszewska, A. Walther, J.-M. Malho, F. H. Schacher, J. Ruokolainen, M. Ankerfors, J. Laine, L. A. Berglund, M. Osterberg and O. Ikkala, Biomacromolecules, 2011, 12, 2074–2081.
24 J. K. Jackson, K. Letchford, B. Z. Wasserman, L. Ye, W. Y. Hamad and H. M. Burt, Int. J. Nanomed., 2011, 6, 321–330.
25 H. Wang and M. Roman, Biomacromolecules, 2011, 12, 1585–1593.
26 K. A. Mahmoud, K. B. Male, S. Hrapovic and J. H. T. Luong, ACS Appl. Mater. Interfaces, 2009, 1, 1383–1386.
27 X. Dang, H. Yi, M.-H. Ham, J. Qi, D. S. Yun, R. Ladewski, M. S. Strano, P. T. Hammond and A. M. Belcher, Nat. Nanotechnol., 2011, 6, 377–384.
28 C.-Y. Chiang, J. Epstein, A. Brown, J. N. Munday, J. N. Culver and S. Ehrman, Nano Lett., 2012, 12, 6005–6011.
29 S. Bolisetty, J. Adamcik, J. Heier and R. Mezzenga, Adv. Funct. Mater., 2012, 22, 3424–3428.
30 E. Royston, A. Ghosh, P. Kofinas, M. T. Harris and J. N. Culver, Langmuir, 2008, 24, 906–912.
31 L. Hu, N. Liu, M. Eskilsson, G. Zheng, J. McDonough, L. Wågberg and Y. Cui, Nano Energy, 2013, 2, 138–145.
32 J. Huang, H. Zhu, Y. Chen, C. Preston, K. Rohrbach, J. Cumings and L. Hu, ACS Nano, 2013, DOI: 10.1021/nn304407r.

33 P. Atanasova and D. Rothenstein, *Adv. Mater.*, 2011, **23**, 4918–4922.

34 C. Li, J. Adamcik and R. Mezzenga, *Nat. Nanotechnol.*, 2012, **7**, 421–427.

35 C. Li and R. Mezzenga, *Langmuir*, 2012, **28**, 10142–10146.

36 T. Zhang, W. Wang, D. Zhang, X. Zhang, Y. Ma, Y. Zhou and L. Qi, *Adv. Funct. Mater.*, 2010, **20**, 1152–1160.

37 W. Wang, T.-J. Zhang, D.-W. Zhang, H.-Y. Li, Y.-R. Ma, L.-M. Qi, Y.-L. Zhou and X.-X. Zhang, *Talanta*, 2011, **84**, 71–77.

38 R. T. Olsson, M. A. S. Azizi Samir, G. Salazar-Alvarez, L. Belova, V. Ström, L. A. Berglund, O. Ikkala, J. Nogués and U. W. Gedde, *Nat. Nanotechnol.*, 2010, **5**, 584–588.

39 J. Wang, Y. Zhu and J. Du, *J. Mech. Med. Biol.*, 2011, **11**, 285–306.

40 O. G. Jones and R. Mezzenga, *Soft Matter*, 2012, **8**, 876.

41 G. H. Altman, F. Diaz, C. Jakuba, T. Calabro, R. L. Horan, J. Chen, H. Lu, J. Richmond and D. L. Kaplan, *Biomaterials*, 2003, **24**, 401–416.

42 T. G. Kim, H. Shin and D. W. Lim, *Adv. Funct. Mater.*, 2012, **22**, 2446–2468.

43 Q. Lu, X. Wang, S. Lu, M. Li, D. Kaplan and H. Zhu, *Biomaterials*, 2011, **32**, 1059–1067.

44 J. A. P. de Mesquita, P. S. Patrício, C. L. Donnici, D. F. S. Petri, L. C. A. de Oliveira and F. V. Pereira, *Soft Matter*, 2011, **7**, 4405.

45 J. Wang, Y. Wan, J. Han, X. Lei, T. Yan and C. Gao, *Micro Nano Lett.*, 2011, **6**, 133.

46 J. Wang, Y. Wan, H. Luo, C. Gao and Y. Huang, *Mater. Sci. Eng., C*, 2012, **32**, 536–541.

47 A. Orza, O. Soritau, L. Olenic, M. Diudea, A. Florea, D. Rus Ciuca, C. Mihu, D. Casciano and A. S. Biris, *ACS Nano*, 2011, **5**, 4490–4503.

48 S. Arola, T. Tammelin, H. Setälä, A. Tullila and M. B. Linder, *Biomacromolecules*, 2012, **13**, 594–603.

49 C.-N. Wu, T. Saito, S. Fujisawa, H. Fukuzumi and A. Isogai, *Biomacromolecules*, 2012, **13**, 1927–1932.

50 C. Aulin, G. Salazar-Alvarez and T. Lindström, *Nanoscale*, 2012, **4**, 6622–6628.

51 T. T. T. Ho, T. Zimmermann, S. Ohr and W. R. Caseri, *ACS Appl. Mater. Interfaces*, 2012, **4**, 4832–4840.

52 J. Cai, S. Liu, J. Feng, S. Kimura, M. Wada, S. Kuga and L. Zhang, *Angew. Chem., Int. Ed.*, 2012, **51**, 2076–2079.

53 C. Schütz, J. Sort, Z. Bacsik, V. Oliynyk, E. Pellicer, A. Fall, L. Wågberg, L. Berglund, L. Bergström and G. Salazar-Alvarez, *PLoS One*, 2012, **7**, e45828.

54 E. Kharlampieva, V. Kozlovskaya, B. Wallet, V. V. Shevchenko, R. R. Naik, R. Vaia, D. L. Kaplan and V. V. Tsukruk, *ACS Nano*, 2010, **4**, 7053–7063.

55 P. Laaksonen, A. Walther, J.-M. Malho, M. Kainlauri, O. Ikkala and M. B. Linder, *Angew. Chem., Int. Ed.*, 2011, **50**, 8688–8691.

56 L.-N. Niu, L. Jiao, Y.-P. Qi, C. K. Y. Yiu, H. Ryou, D. D. Arola, J.-H. Chen, L. Breschi, D. H. Pashley and F. R. Tay, *Angew. Chem., Int. Ed.*, 2011, **50**, 11688–11691.

57 M. Kettunen, R. J. Silvennoinen, N. Houbenov, A. Nykänen, J. Ruokolainen, J. Sainio, V. Pore, M. Kemell, M. Ankerfors, T. Lindström, M. Ritala, R. H. A. Ras and O. Ikkala, *Adv. Funct. Mater.*, 2011, **21**, 510–517.

58 P. Thanikaivelan, N. T. Narayanan, B. K. Pradhan and P. M. Ajayan, *Sci. Rep.*, 2012, **2**, 230.

59 C. Aimé, G. Mosser, G. Pembouong, L. Bouteiller and T. Coradin, *Nanoscale*, 2012, **4**, 7127–7134.

60 K. E. Shopsowitz, H. Qi, W. Y. Hamad and M. J. Maclachlan, *Nature*, 2010, **468**, 422–425.

61 F. Vollrath and D. P. Knight, *Nature*, 2001, **410**, 541–548.

62 P. Fratzl, *Curr. Opin. Colloid Interface Sci.*, 2003, **8**, 32–39.

63 W.-J. Chung, J.-W. Oh, K. Kwak, B. Y. Lee, J. Meyer, E. Wang, A. Hexemer and S.-W. Lee, *Nature*, 2011, **478**, 364–368.

64 S. Beck-Candanedo, M. Roman and D. G. Gray, *Biomacromolecules*, 2005, **6**, 1048–1054.

65 K. E. Shopsowitz, W. Y. Hamad and M. J. MacLachlan, *Angew. Chem., Int. Ed.*, 2011, **50**, 10991–10995.

66 C. Olivier, C. Moreau, P. Bertoncini, H. Bizot, O. Chauvet and B. Cathala, *Langmuir*, 2012, **28**, 12463–12471.

67 Y. Fan, T. Saito and A. Isogai, *Biomacromolecules*, 2008, **9**, 1919–1923.

68 K. Ariga, *Manipulation of Nanoscale Materials*, Royal Society of Chemistry, Cambridge, 2012.

69 K. Ariga, M. Li, G. J. Richards and J. P. Hill, *J. Nanosci. Nanotechnol.*, 2011, **11**, 1–13.

70 A. P. Mangalam, J. Simonsen and A. S. Benight, *Biomacromolecules*, 2009, **10**, 497–504.

71 H. Yi, G. W. Rubloff and J. N. Culver, *Langmuir*, 2007, **23**, 2663–2667.

72 P. W. K. Rothemund, *Nature*, 2006, **440**, 297–302.

73 F. A. Aldaye, A. L. Palmer and H. F. Sleiman, *Science*, 2008, **321**, 1795–1799.

74 S. Deville, *Adv. Eng. Mater.*, 2008, **10**, 155–169.

5478 | *J. Mater. Chem. A*, 2013, **1**, 5469–5478

This journal is © The Royal Society of Chemistry 2013